J Ther Eng, Vol. 10, No. 4, pp. 836−846, July, 2024

Journal of Thermal Engineering
Web page info: https://jten.yildiz.edu.tr
DOI: 10.14744/thermal.0000835

Research Article

Dynamics of thermal radiation and heat generation/absorption on a viscous MHD micropolar fluid over a stretching sheet with suction/injection

C. A. ADEYEMI[1], B. I. OLAJUWON[1], B. J. AKINBO[1,*], M. T. RAJI[1]

[1]*Department of Mathematics, Federal University of Agriculture, Abeokuta, 2240, Nigeria*

ARTICLE INFO

Article history
Received: 17 April 2023
Revised: 28 October 2023
Accepted: 30 October 2023

Keywords:
Galerkin Weighted Residual; Heat Generation/Absorption; Micropolar Fluid; Thermal Radiation; Viscous Dissipation

ABSTRACT

This paper, analysed by computation, the behaviour of thermal radiation and heat generation/absorption in a viscous Magnetohydrodynamics Micropolar fluid through a porous medium of a stretching sheet with suction/injection. The investigation is done using the set of coupled nonlinear partial differential equations that describe the dynamics of the flow and heat transfer. These equations are transformed into a system of ordinary differential equations which are solved via the Galerkin Weighted Residual method. The behaviour of various embedded parameters adopted was presented graphically and discussed through tables accordingly. Aside from other major findings, the novel result shows that microrotation is a decreasing function of Magnetic and porosity parameters while increasing values of heat generation magnify the fluid molecules and strengthen the thermal effect on fluid at a far field. Also, higher variation of coupling constant depicts a lower viscosity nature and reduces the rotation of the fluid molecules. The validation obtained agreed with the literature.

Cite this article as: Adeyemi CA, Olajuwon BI, Akinbo BJ, Raji MT. Dynamics of thermal radiation and heat generation/absorption on a viscous MHD micropolar fluid over a stretching sheet with suction/injection. J Ther Eng 2024;10(4):836−846.

INTRODUCTION

The study of micropolar fluid has been a popular research area for many years. Goud [1] explained that it is an area of interest to many researchers because of the extensive relevance of micropolar fluids to technology. The solution of the governing equation responsible for the flow and heat transfer are solved by different methods in the literature among which are Shooting Method, Weighted Residual and Adomial Decomposition, among others. Micropolar fluids represent fluids consisting of rigid randomly oriented particles suspended in a viscous medium, where the deformation of particles is ignored. It is a subclass of microfluids as simplified and defined by Erigen [2, 3]. Erigen's theory can be used to study how liquid crystals, polymeric fluids and exotic lubricants behave. There are lots of industrial processes that require fluid as a working medium. This prompted Ariman et al. [4] to do a review of micropolar fluids and discussed how it can be applied to technology. Nadeem et al. [5] studied how an unsteady biconvection nanomaterial Micropolar fluid behaves over an exponentially stretching surface when subject to multi slip conditions. The results show that the fluid temperature

*Corresponding author.
*E-mail address: akinbomaths@gmail.com

This paper was recommended for publication in revised form by Editor-in-Chief Ahmet Selim Dalkılıç

gained strength with the smaller values of the Prandt than the higher values. Damseh et al. [6] examined natural convection heat and mass transfer adjacent to a continuously moving vertical permeable infinitely long surface for incompressible micropolar fluid in the presence of heat generation/absorption with the first-order chemical reaction. It was reported that heat and mass transfer coefficients are enhanced with a rise in the heat generation/absorption and the chemical reaction parameters. Damseh [7] researched unsteady natural convection heat and mass transport of micropolar fluid over a vertical surface with constant heat flux where the enhancement in the vortex viscosity was viewed to magnify the rotation within the boundary layer which has a propensity to strengthen the coefficient of friction. Baharifard et al. [8] studied the flow of MHD micropolar over a moving plate with suction and injection boundary conditions.

The impacts of radiation, heat generation, and viscous dissipation play significant roles in both free and forced convection flow and have also caught the attention of researchers. For example, engineering and physics both benefit from the use of radiation. In space technology and high-temperature operations, the effects of thermal radiation heat transfer on various flows are crucial while significant of heat generation/absorption as well as the viscous dissipation which describes how kinetic energy is being transformed into internal energy by work done against viscous stresses, making the process irreversible has been studied in the literature. In research into the unstable case of free convection across an infinite vertical plate in the presence of thermal radiation, Das et al. [9] found that the plate shear stress is marginally larger for uniform heat flux (UHF)than uniform wall temperature (UWT). Koriko et al. [10] reported that the flow near a free stream's temperature distribution is unaffected by thermal stratification while investigating the effects of thermal stratification as well as nonlinear thermal radiation on the behaviour of micropolar fluid along a vertical surface. Magnetic force's effectiveness on ferrofluid's thermal performance in a screw tube was examined by Barzegar Gerdroodbary et al. [11]. Mamun et al. [12] observed that variation in heat generation accelerates the mobility of fluid molecules while investigating the impact of heat generation and viscous dissipation on magnetohydrodynamics natural convection

The presence of permeability in the flow of heat and mass transport cannot be overemphasized as its dynamics play a significant role in Science and Engineering field among which is filtration, as a result of its various importance, a good number of authors have worked on permeability effect in the literature. Postelnicu [13] examined the impact of the magnetic field on the transfer of heat and mass numerically by means of natural convection on vertical surfaces that are porous in nature. The study remarked that the thickness of the hydrodynamics, thermal and concentration layers improve over the strength of magnetic intensity. Haque [14] studied the effects of an induced magnetic field on the transient heat and mass transfer magneto micropolar fluid flow past a semi-infinite vertical plate surrounded by a porous medium in the presence of a constant heat sink. Using the homotopy analysis method, Akinbo and Olajuwon [15, 16] worked on various forms of heat and mass transports in the flow of Walters' B fluid through a porous medium where the random movement of the fluid molecules was found to be resisted by the porosity impact. Reddy et al. [17] investigated mass transfer and radiation effects of unsteady MHD-free convection fluid flow via in porous medium with heat generation/ absorption. Mamta and Krishna [18] studied the effects of radiation absorption, mass diffusion, chemical reaction and heat source of heat generating fluid past a vertical porous plate subjected to variable suction with the assumption that the plate is embedded in a uniform porous medium and moves with a constant velocity in the flow direction in the presence of a transverse magnetic field.

Other areas of fluid dynamics that are also essential for the current trend of scientific development aside from the Micropolar fluid have also been considered in the literature. Joshi et al. [19-22] investigated via horizontal pipeline the Slurry flow characteristics at various Prandtl numbers as well as other investigations involving transportation in a straight pipe where the Maximum specific energy consumption for each particle and efflux is shown by the fluid at increasing Prandtl numbers among others findings. Parkash et al. [23] buttressed that suspension stability enhancement is significant for the lower Prandtl number range and diminishes for the higher Prandtl number range while investigating various values of Prandt numbers CFD modeling of the slurry pipeline.

Motivated by the existing work in the literature and the application of the micropolar fluid in science related disciplines, this work aims to provide more insight into the field by considering the behaviors of heat generation/absorption in an extension to the work in Baharifard et al. [8]. The objective is to examine the combined impact of thermal radiation and heat generation/absorption on a viscous Micropolar fluid over a stretching sheet with suction/injection.

PROBLEM FORMULATION

Consider a steady case of two-dimensional boundary layers' transport of a magnetohydrodynamics Micropolar fluid through a porous medium of a horizontal stretching sheet with suction/injection. The fluid exhibits the constant properties of a viscous fluid and the magnetic field B_o of uniform strength is executed in a perpendicular direction to the flow as shown in Figure 1. On the account of the small magnetic Reynolds number, the induced magnetic parameter is negligible. No electric field is assumed to exist and the hall effect is not taken into account. The heat transport is considered with the combined impact of thermal radiation, viscous dissipation and heat generation/absorption.

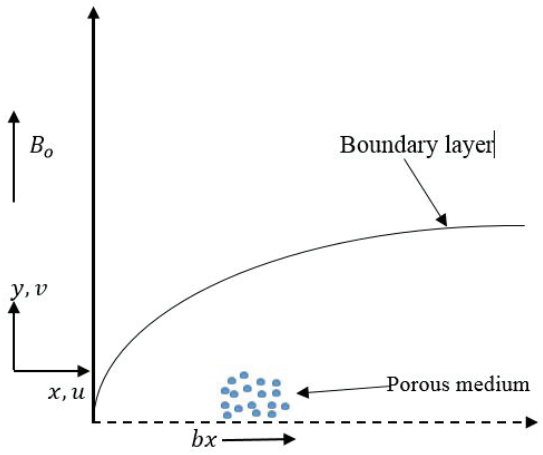

Figure 1. Model geometry.

The fluid temperature is taken as T while the surface and ambient temperatures are denoted by T_w and T_∞. Velocity of the stretching sheet is taken as $u_w(x) = bx$.

Taking into account the aforementioned expression, the model equations for transport phenomena under the usual boundary layer approximation are stated for continuity, momentum, microrotation, and energy equations (Baharifard et al. [8], Sedeek et al. [24]) respectively as follows

$$\frac{\partial u}{\partial x}+\frac{\partial v}{\partial y}=0 \tag{1}$$

$$u\frac{\partial u}{\partial x}+v\frac{\partial u}{\partial y}=v\frac{\partial^2 u}{\partial y^2}+\mathrm{k}_1\frac{\partial N}{\partial y}-\frac{\sigma {B_o}^2}{\rho_\infty}u-\frac{\nu}{K}u \tag{2}$$

$$\mathrm{G}_1\frac{\partial^2 N}{\partial y^2}-2N-\frac{\partial u}{\partial y}=0 \tag{3}$$

$$u\frac{\partial T}{\partial x}+v\frac{\partial T}{\partial y}=\frac{k}{\rho \mathrm{c}_p}\frac{\partial^2 T}{\partial y^2}-\frac{k}{\rho \mathrm{C}_p}\frac{\partial \mathrm{q}_r}{\partial y}+\frac{v}{\mathrm{C}_p}\left(\frac{\partial u}{\partial y}\right)^2+\frac{Q_o}{\rho C_p}(T-T_\infty) \tag{4}$$

The boundary conditions are:

$$u_w(x)=bx,\ v=v_w,\ N=0, T=T_w, at\ y=0, \tag{5}$$

$$u\to 0,\quad N\to 0,\quad T\to T_\infty, at\ y\to\infty \tag{6}$$

Velocities in x and y directions are *u and v respectively*, v_w is velocity of suction/injection at the wall, b is a constant, ν is the kinematic viscosity, K is the permeability of porous medium, N represents microrotation, σ is the electrical conductivity. The coupling constant $k_1=\frac{s}{\rho}$ where s is a constant characteristic of the fluid and ρ is the density of the fluid. G_1 is the microrotation constant, Q_o is the heat generation/absorption coefficient, k is the thermal conductivity, C_p is the specific heat of the fluid at constant pressure and ∞ describes far field condition. Since the boundary layer is optically thick, the Rosseland approximation for heat transport is taken into consideration. The radiative heat flux $\mathrm{q}_r=-\frac{4\sigma^*\partial T^4}{3k^*\partial y}$ (σ^* and k^* are the Stefan-Boltzmann constant and the mean absorption coefficient, respectively).

Assuming temperature varies as the flow progresses, we linearize by using the Taylor's series to expand the term T^4 about T_∞. Therefore $T^4\approx 4T_\infty^3T-3T_\infty^4$ (overlooking the higher order parts).

Applying the transformation techniques components expressed below

$$\eta=b^{\frac{1}{2}}\nu^{-\frac{1}{2}}y,\psi=(\mathrm{bv})^{\frac{1}{2}}\mathrm{xf}\,(\eta),N=b^{\frac{3}{2}}\nu^{-\frac{1}{2}}\mathrm{xg}(\eta),\ \theta(\eta)=\frac{T-T_\infty}{T_w-T_\infty}$$

results in dimensionless equations (7) to (9)

$$f'''(\eta)+f(\eta)f''(\eta)-\left(f'(\eta)\right)^2-(M+P)f'(\eta)+Kg'(\eta)=0 \tag{7}$$

$$Gg''(\eta)-(2g(\eta)+f''(\eta))=0 \tag{8}$$

$$\left(\frac{1+R}{RPr}\right)\theta''(\eta)+f(\eta)\theta'(\eta)-\gamma f'(\eta)\theta(\eta)+Ec(f''(\eta))^2+Q\theta(\eta)=0 \tag{9}$$

And the boundary conditions on a semi-infinite computational domain is as follows

$$f(0)=F_w,\quad f'(0)=1,\quad f'(\infty)=0,\quad g(0)=0,\quad g(\infty)=0,\quad \theta(0)=1,\quad \theta(\infty)=0 \tag{10}$$

Some important physical parameters applied are:

$$\text{Prandtl number}\quad \mathrm{Pr}=\frac{\rho \mathrm{c}_p\nu}{k},$$

$$\text{Magnetic field parameter}\quad M=\frac{\sigma {\mathrm{B}_o}^2}{\rho_\infty b}$$

$$\text{Coupling constant parameter}\quad K=\frac{k_1}{\nu},$$

$$\text{Microrotation number}\quad G=\frac{G_1 b}{\nu}$$

$$\text{Eckert number} \quad \text{Ec} = \frac{{u_w}^2}{\text{C}_p(T_w - T_\infty)},$$

$$\text{Permeability parameter } P = \frac{\upsilon}{kb},$$

$$\text{Heat generation/absorption} = \frac{Q_o \upsilon}{\rho \text{C}_p b},$$

$$\text{Suction/Injection parameter } F_w = \frac{-v_w}{\sqrt{b\upsilon}}$$

Method of Solution

Differential equations are generally inevitable in the field of applied Mathematics. Their solutions can be obtained by several methods. Here, Galerkin Weighted Residual Method (GWRM) is adopted for this work as it is very efficient in providing accurate result for non-linear differential equations. Following Akinbo and Olajuwon [25], Eqs. (7) - (9) and (10), followed from trial functions.

$$f(\eta) = \sum_{i=0}^{12} a_i e^{\frac{i\eta}{4}}, \quad g(\eta) = \sum_{i=1}^{13} b_i e^{\frac{i\eta}{4}}, \quad \theta(\eta) = \sum_{i=1}^{13} c_i e^{\frac{i\eta}{4}} \tag{11}$$

applying the boundary conditions (10), gives

$$a_0 + a_1 + a_2 + a_3 + a_4 + a_5 + a_6 + a_7 + a_8 + a_9 + a_{10} + a_{11} + a_{12} - f_w = 0 \tag{12}$$

$$b_1 + b_2 + b_3 + b_4 + b_5 + b_6 + b_7 + b_8 + b_9 + b_{10} + b_{11} + b_{12} + b_{13} = 0 \tag{13}$$

$$c_1 + c_2 + c_3 + c_4 + c_5 + c_6 + c_7 + c_8 + c_9 + c_{10} + c_{11} + c_{12} + c_{13} - 1 = 0 \tag{14}$$

while $f'(0) = 1$, results in

$$-\frac{1}{4}a_1 - \frac{1}{2}a_2 - \frac{3}{4}a_3 - a_4 - \frac{5}{4}a_5 - \frac{3}{2}a_6 - \frac{7}{4}a_7 - 2a_8 - \frac{9}{4}a_9 - \frac{5}{2}a_{10} - \frac{11}{4}a_{11} - 3a_{12} - 1 = 0 \tag{15}$$

The unbounded interval $f(\infty)$, $g(\infty)$ *and* $\theta(\infty)$ automatically agreed. Following the rule of the solution, the functions expressed in Eqn. (11) and non-dimensional eqns. (7 - 9) produce the residual functions R_f, R_g and R_θ multiplied by $e^{-\frac{j}{4}\eta}\ \forall\ j \in \mathbb{Z}$ and integrated under the associated boundary conditions which were carried out through MATHEMATICA package

RESULTS AND DISCUSSION

In order to gain physical understanding to the study, the embedded parameters: $R = 0.1$, $P = 1$, $G = 2$, $K = 1$, $\gamma = 1$, $Ec = 0.02$, $Pr = 5.2$, $F_w = 0.1$, $Q = 0.02$ are discussed by varying each parameter while keeping the others constant. Tables 1–5 demonstrated agreement with the existing literature when compared with Sedeek et al. [24] and Baharifard et al. [8] for skin fiction $f''(0$, wall couple stress $g'(0)$ and Nusselt number $\theta'(0)$.

Table 6 presents the behaviours of various parameters on skin friction, wall couple stress and Nusselt number.

Table 1. Prandtl number for $f''(0)$, $g'(0)$, $\theta'(0)$

Pr	Analytical by Seddeek et al. [24]	Numerical by Seddeek et al. [24]	RGT by Baharifard et al. [8]	EGT by Baharifard et al. [8]	Present result
$f''(0)$					
0.71	-1.67662	-1.67631	-1.67635	-1.67631	-1.67631
5	-1.67662	-1.67631	-1.67635	-1.67631	-1.67631
10	-1.67662	-1.67631	-1.67635	-1.67631	-1.67631
$g'(0)$					
0.71	0.310602	0.317949	0.317946	0.317949	0.317949
5	0.310602	0.317949	0.317946	0.317949	0.317949
10	0.310602	0.317949	0.317946	0.317949	0.317949
$\theta'(0)$					
0.71	-0.50758	-0.50057	-0.47829	-0.47826	-0.47830
5	-1.94846	-1.95000	-3.89998	-1.95000	-1.95000
10	-2.93323	-2.93284	-2.92898	-2.93283	-2.93283

Table 2. Magnetic parameter for $f''(0)$, $g'(0)$, $\theta'(0)$

Mn	Analytical by Seddeek et al. [24]	Numerical by Seddeek et al. [24]	RGT by Baharifard et al. [8]	EGT by Baharifard et al. [8]	Present result
$f''(0)$					
1	-1.358082	-1.358217	-1.360011	-1.358217	-1.358217
2	-1.676622	-1.676305	-1.67635	-1.676305	-1.676305
3.8	-2.138957	-2.138018	-2.137928	-2.138018	-2.138021
$g'(0)$					
1	0.283562	0.294877	0.294868	0.294877	0.294877
2	0.310602	0.317949	0.317946	0.317949	0.317949
3.8	0.339333	0.343713	0.343713	0.343713	0.343713
$\theta'(0)$					
1	-3.033721	-3.034414	-3.027976	-3.034371	-3.034404
2	-2.933228	-2.932841	-2.928977	-2.932825	-2.932831
3.8	-2.779171	-2.779855	-2.779873	-2.781256	-2.781248

Table 3. Coupling constant parameter for $f''(0)$, $g'(0)$, $\theta'(0)$

K	Analytical by Seddeek et al. [24]	Numerical by Seddeek et al. [24]	RGT by Baharifard et al. [8]	EGT by Baharifard et al. [8]	Present result
$f''(0)$					
1	-1.676622	-1.676305	-1.67635	-1.676305	-1.676305
4	-1.493959	-1.49467	-1.498385	-1.49467	-1.494670
$g'(0)$					
1	0.310602	0.317949	0.317946	0.317949	0.317949
4	0.325028	0.321999	0.321966	0.321999	0.321999
$\theta'(0)$					
1	-2.933228	-2.932841	-2.928977	-2.932825	-2.932831
4	-2.973965	-2.974663			-2.965156

Table 4. Thermal radiation parameter for $f''(0)$, $g'(0)$, $\theta'(0)$

R	Analytical by Seddeek et al. [24]	Numerical by Seddeek et al. [24]	RGT by Baharifard et al. [8]	EGT by Baharifard et al. [8]	Present Result
$f''(0)$					
0.1	-1.676622	-1.676305	-1.67635	-1.676305	-1.676305
0.5	-1.676622	-1.676305	-1.67635	-1.676305	-1.676305
1	-1.676622	-1.676305	-1.67635	-1.676305	-1.676305
3	-1.676622	-1.676305	-1.67635	-1.676305	-1.676305
$g'(0)$					
0.1	0.310602	0.317949	0.317946	0.317949	0.317949
0.5	0.310602	0.317949	0.317946	0.317949	0.317949
1	0.310602	0.317949	0.317946	0.317949	0.317949
3	0.310602	0.317949	0.317946	0.317949	0.317949
$\theta'(0)$					
0.1	-0.719536	-0.742685	-0.737100	-0.737100	-0.737000
0.5	-1.807747	-1.813284	-1.813271	-1.813283	-1.813283
1	-2.317869	-2.318467	-2.318089	-2.318462	-2.318460
3	-2.933228	-2.932841	-2.928977	-2.932825	-2.932831

Table 5. Suction/Injection parameter for $f''(0)$, $g'(0)$, $\theta'(0)$

Fw	Analytical by Seddeek et al. [24]	Numerical by Seddeek et al. [24]	RGT by Baharifard et al. [8]	EGT by Baharifard et al. [8]	Present Result
$f''(0)$					
-0.5	-1.434341	-1.444333	-1.445684	-1.444294	-1.444333
0	-1.676622	-1.676305	-1.676350	-1.676305	-1.676305
0.5	-1.940262	-1.946052	-1.945493	-1.946015	-1.946052
$g'(0)$					
-0.5	0.292893	0.300334	0.300312	0.300334	0.300334
0	0.310602	0.317949	0.317946	0.317949	0.317949
0.5	0.327805	0.334831	0.334828	0.334831	0.334831
$\theta'(0)$					
-0.5	-1.398473	-1.392094	-1.39209	-1.392087	-1.392089
0	-2.933228	-2.932841	-2.928977	-2.932825	-2.932830
0.5	-5.528042	-5.52773	-5.558338	-5.526077	-5.527739

Obviously from the table, the skin friction produced negative values, indicating the presence of a drag force exerted on the fluid by the plate. However, the Prandtl number and radiation parameter are increasing functions of the Nusselt number which enhances the rate of heat transfer.

Figures 2 and 3 illustrate the behaviour of magnetic parameter (M) via velocity field $f'(\eta)$ and Rotational velocity profile $g(\eta)$. As expected, a drag-like force known as Lorentz force that opposes the fluid motion is produced by an increase in M causing a reduction in the velocity and microrotation velocity of the fluid. This in turn results in a decrease of the momentum boundary layer thickness. The reverse is the case as observed in Figure 4 where an advancement in the value of the magnetic parameter led to frictional heating which contributed to a higher temperature distribution within the layer that consequently increased the thickness of the thermal boundary layer. Figures 5 and 6 illustrate the behaviour of the permeability parameter (P) via $f'(\eta)$ and $g(\eta)$. As expected, an increase in P produces a high resistance to the velocity distribution of the fluid thereby causing a reduction in $f'(\eta)$ and $g(\eta)$. The resistance against the motion of the fluid particles pioneer

Table 6. Skin friction, wall couple stress and Nusselt number with $\gamma = 1.0$

P	Pr	R	Ec	G	Q	K	M	$f''(0)$	$g'(0)$	$-\theta'(0)$
0.1								-1.444300	0.302006	0.488840
1.0	5.2	0.1	0.02	2.0	0.02	1.0	1.0	-1.72724	0.321402	0.434851
2.0								-1.996517	0.336749	0.389206
	2.5							-1.727238	0.321402	0.206549
	3.2							-1.727238	0.321402	0.268850
		0.5						-1.727241	0.321402	1.266459
		1.5						-1.727241	0.321402	1.905972
			2.0					-1.727241	0.321402	-0.340982
			4.0					-1.727241	0.321402	-1.124651
				1.0				-1.698712	0.560705	0.427601
				3.0				-1.740223	0.229179	0.438044
					2.0			-1.727217	0.321404	1.387059
					4.0			-1.727277	0.321400	1.537771
						2.0		-1.669589	0.322654	0.421231
						3.0		-1.609523	0.324128	0.404296
							2.0	-1.996517	0.336749	0.389206
							3.0	-2.234177	0.348305	0.353071

heating by means of the viscosity of the fluid that aftermath improve $\theta(\eta)$ as shown in Figure 7, thereby causing an increase of the thermal boundary layer thickness.

When the coupling constant parameter K is increased, Figures 8 and 9 show that K is a decreasing function of velocity field and micro rotation. This phenomenon corresponds to the position of the viscosity as its higher variation of K depicts a lower viscosity nature, and reduces the rotation of the fluid molecules, thereby causing a decrease in the momentum boundary layer thickness. This outcome

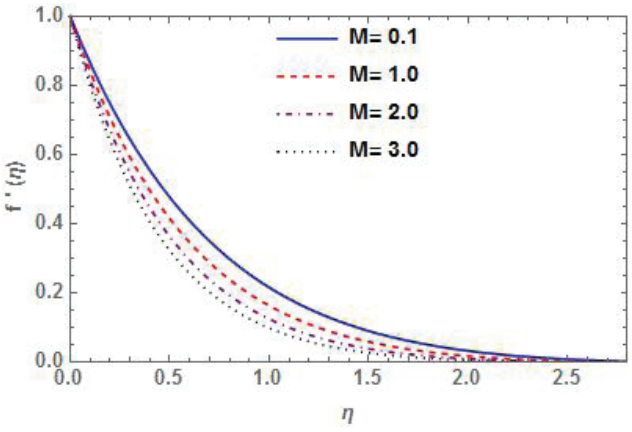

Figure 2. $f'(\eta)$ versus M.

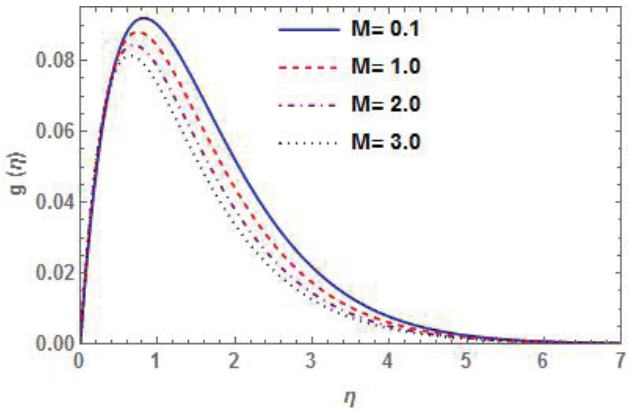

Figure 3. $g(\eta)$ versus M.

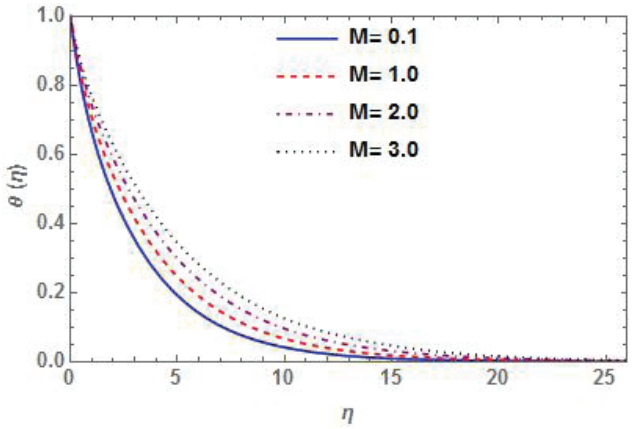

Figure 4. $\theta(\eta)$ versus M.

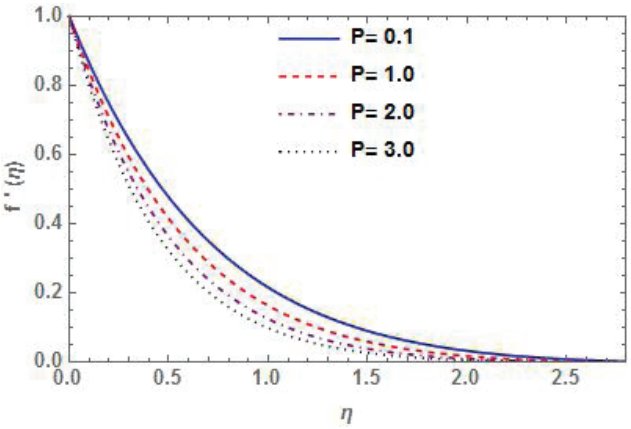

Figure 5. $f'(\eta)$ versus P.

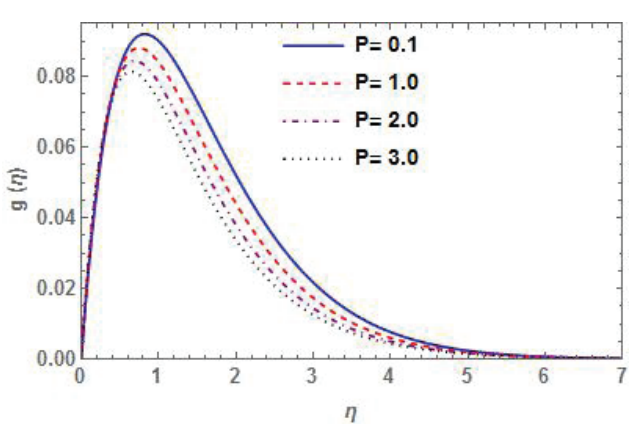

Figure 6. $g(\eta)$ versus P.

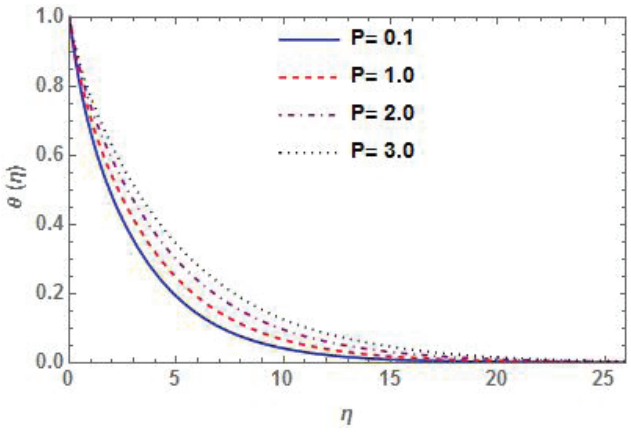

Figure 7. $\theta(\eta)$ versus P.

agreed with Baharifard et al. [8], with a reverse phenomenon on temperature field as shown in Figure 10 where an increase in K raises the temperature distribution and its associated thermal boundary layer thickness. Figures 11–13 show the movement of the fluid, the microrotation velocity and the temperature of the fluid towards the boundary of the plate due to the presence of the suction/injection parameter. This causes the layer thickness to reduce. It is important to note that permeability impact on the stretching sheet with suction is sometimes applied to avoid the separation of the boundary layer. This phenomenon agreed with Hayat et al. [26].

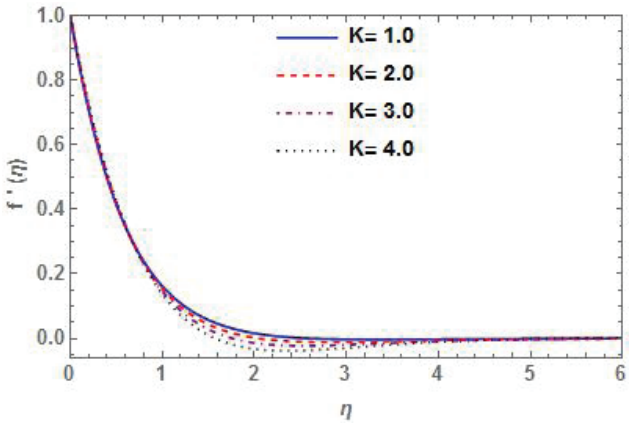

Figure 8. $f'(\eta)$ versus K.

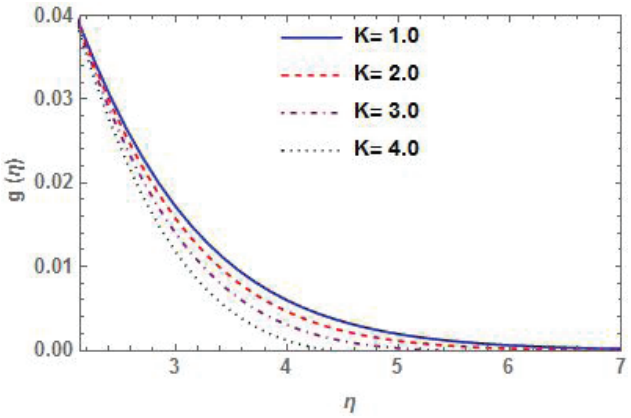

Figure 9. $g(\eta)$ versus K.

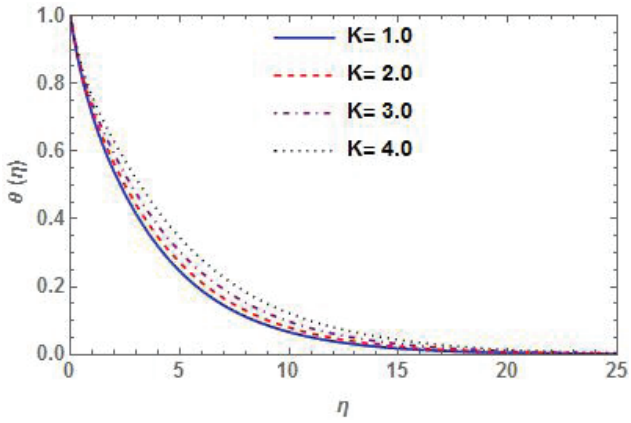

Figure 10. $\theta(\eta)$ versus K.

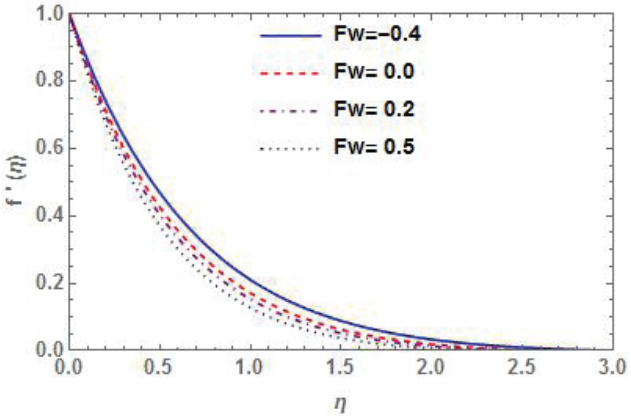

Figure 11. $f'(\eta)$ versus F_w.

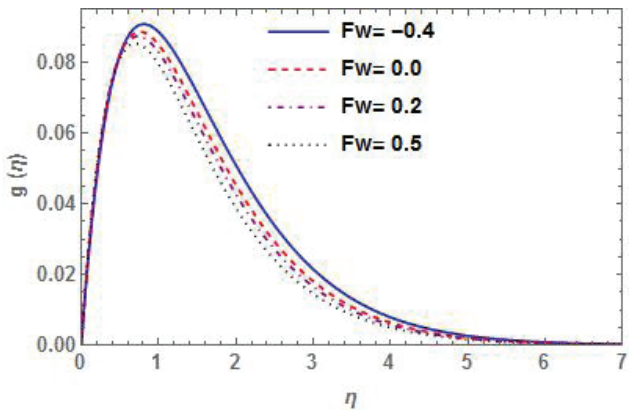

Figure 12. $g(\eta)$ versus f_w.

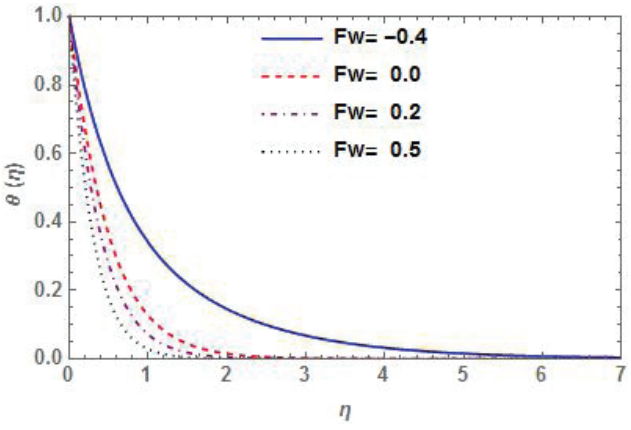

Figure 13. $\theta(\eta)$ versus f_w.

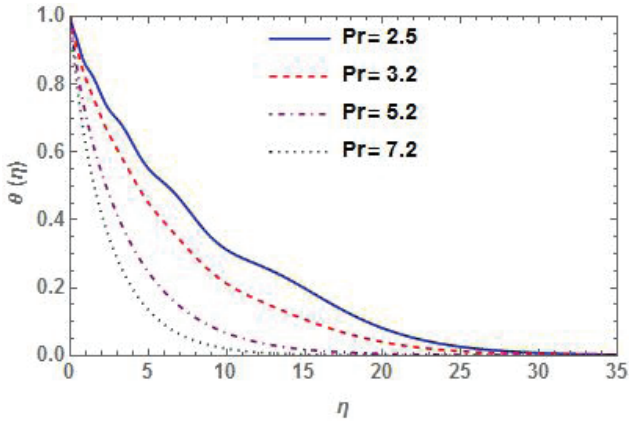

Figure 14. $\theta(\eta)$ versus Pr.

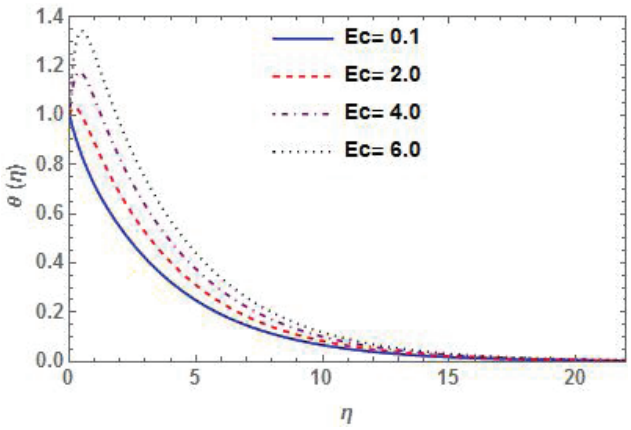

Figure 15. $\theta(\eta)$ versus Ec.

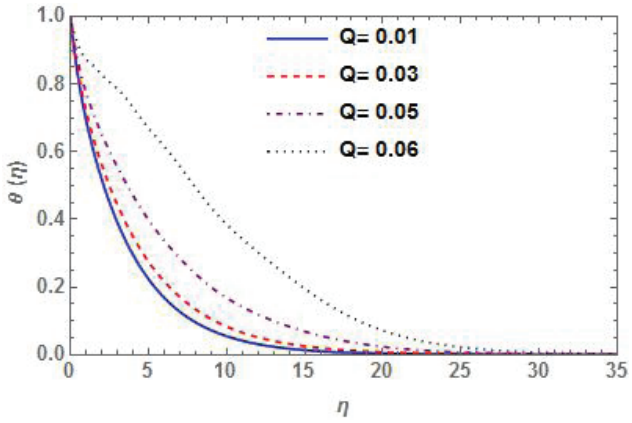

Figure 16. $\theta(\eta)$ versus Q.

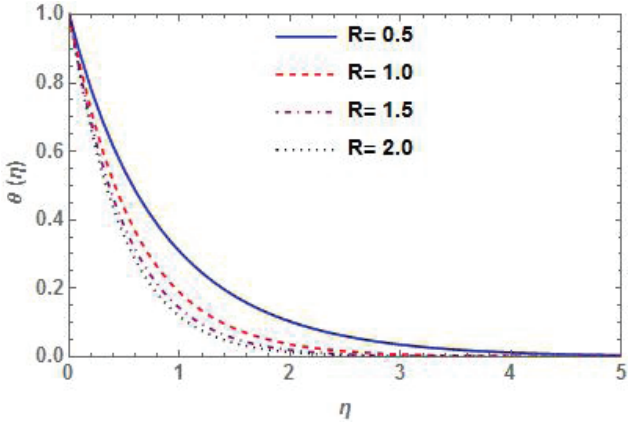

Figure 17. $\theta(\eta)$ versus R.

It is observed from Figure 14 over the low thermal diffusivity that an increase in Pr(*with Pr* > 1) strengthens the convection over conduction and decays the temperature field $\theta(\eta)$ as well as its thermal boundary layer thickness. Thus, at small values of (Pr), the fluid is more conductive than at higher values. An increase in Eckert number (*Ec*) as shown in Figure 15 intensifies the conversion rate of kinetic energy to internal energy which heats up the fluid near the surface. This leads to the release of additional heat generated from friction making the temperature field increase and consequently expanding the thermal boundary layer thickness. These results agreed with Akinbo and Olajuwon [25].

Figure 16 shows that higher temperature is inevitable as Heat generation parameter vary to boost the temperature field within the boundary layer. This automatically produces more heat within the boundary layer which stimulates the fluid molecules and enhances thermal boundary layer thickness. This outcome enables the thermal effect on fluids at the far field. The effect of radiation parameter R on the temperature field is presented in Figure 17. An increase in R precedes a reduction in the rate of energy transport to the fluid (due to the position of $\frac{3kk^*}{16\sigma^* T_\infty{}^3}$) [25]. This outcome ultimately reduces the temperature field and the thermal boundary layer thickness.

CONCLUSION

In this work, analytical techniques have been carried out via the Galerkin Weighted Residual method to investigate the combined impact of thermal radiation and heat generation/absorption on a viscous hydromagnetic micropolar fluid and the following results are generated out of the results obtained.

1. Fluid molecules move more rapidly in their random manner at lower variation in Q at $0.01 \leq Q \leq 0.06$, but get escalated as $Q > 0.06$. This makes the thermal effect have a greater impact on the fluids in distant fields.
2. Microrotation is a decreasing function of Magnetic and porosity parameters as $M, P \in [0.1,3.0]$.
3. The temperature field is boosted over a conversion rate of kinetic energy to internal energy that invokes heat addition by means of frictional heating as $0.1 \leq Q \leq 6.0$

4. Greater resistance is produced against the motion of the fluid on the variation of the porosity parameter, which declines its associated boundary layer thickness.
5. Different values of the Prandtl number and Eckert number improve the Nusselt number which consequently strengthens the rate of heat transfer.

AUTHORSHIP CONTRIBUTIONS

Authors equally contributed to this work.

DATA AVAILABILITY STATEMENT

The authors confirm that the data that supports the findings of this study are available within the article. Raw data that support the finding of this study are available from the corresponding author, upon reasonable request.

CONFLICT OF INTEREST

The author declared no potential conflicts of interest with respect to the research, authorship, and/or publication of this article.

ETHICS

There are no ethical issues with the publication of this manuscript.

REFERENCES

[1] Goud BS. Heat generation/absorption influence on steady stretched permeable surface on MHD flow of a micropolar fluid through a porous medium in the presence of variable suction/injection. Int J Thermofluids 2020;7-8:100044. [CrossRef]
[2] Eringen AC. Simple microfluids. Int J Engineer Sci 1964;2:205−217. [CrossRef]
[3] Eringen AC. Theory of micropolar fluids. J Math Mech 1966;16:1−18. [CrossRef]
[4] Ariman TM, Turk MA, Sylvester ND. Microcontinuum fluid mechanics-a review. Int J Eng Sci 1973;11:905−930. [CrossRef]
[5] Nadeem S, Khan MN, Abbas N. Transportation of slip effects on nanomaterial micropolar fluid flow over exponentially stretching. Alex Eng J 2020;59:3443−3450. [CrossRef]
[6] Damseh RA, Al-Odat MQ, Chamkha AJ, Shannak BA. Combined effect of heat generation or absorption and first-order chemical reaction on micropolar fluid flows over a uniformly stretched permeable surface. Int J Therm Sci 2009;48:1658−1663. [CrossRef]
[7] Damseh RA. Unsteady natural convection heat transfer of micropolar fluid over a vertical surface with constant heat flux. Turk J Engineer Environ Sci 2007;31:225−233.
[8] Baharifard F, Parand K, Rashidi MM. Novel solution for heat and mass transfer of a MHD micropolar fluid flow on a moving plate with suction and injection. Engineer Comput 2022;38:13−30. [CrossRef]
[9] Das S, Jana RN, Chamkha AJ. Unsteady free convection flow past a vertical plate with heat and mass fluxes in the presence of thermal radiation. J Appl Fluid Mech 2015;8:845−854. [CrossRef]
[10] Koriko OK, Animasaun IL, Omowaye AJ, Oreyeni T. The combined influence of nonlinear thermal radiation and thermal stratification on the dynamics of micropolar fluid along a vertical surface. Multidiscipline Modeling Mater Struct 2019;15:133−155. [CrossRef]
[11] Barzegar Gerdroodbary M, Jafaryar M, Sheikholeslami M, Amini Y. The efficacy of magnetic force on thermal performance of ferrofluid in a screw tube. Case Stud Therm Engineer 2023;49:103187. [CrossRef]
[12] Mamun AA, Chowdhury ZR, Azim MA, Molla MM. MHD-conjugate heat transfer analysis for a vertical flat plate in presence of viscous dissipation and heat generation. Int Comm Heat Mass Transf 2008;35:1275−1280. [CrossRef]
[13] Postelnicu A. Influence of a magnetic field on heat and mass transfer by natural convection from vertical surfaces in porous media considering Soret and Dufour effects. Int J Heat Mass Transf 2004;47:1467−1472. [CrossRef]
[14] Haque MM. Heat and mass transfer analysis on magneto micropolar fluid flow with heat absorption in induced magnetic field. Fluids 2021;6:126. [CrossRef]
[15] Akinbo BJ, Olajuwon BI. Interaction of radiation and chemical reaction on Walters' B fluid over a medium porosity of a vertical stretching surface. J Heat Transf 2023;52:1689−1709. [CrossRef]
[16] Akinbo BJ, Olajuwon BI. Impact of radiation and heat generation/absorption in a Walters' B fluid through a porous medium with thermal and thermo diffusion in the presence of chemical reaction. Int J Model Simul 2023;43:87−100. [CrossRef]
[17] Reddy GV, Murthy CVR, Reddy NB. Mass transfer and radiation effects of unsteady MHD free convective fluid flow embedded in porous medium with heat generation/absorption. J Appl Comput Math 2010;9:108−113.
[18] Mamta T, Krishna MV. Thermal radiation effect on an unsteady MHD free convective chemically reacting viscous dissipative fluid flow past an infinite vertical moving porous plate with heat source. IOSR J Math 2014;10:89−105. [CrossRef]
[19] Joshi T, Parkash O, Krishan G. CFD modeling for slurry flow through a horizontal pipe bend at different Prandtl number. Int J Hydrogen Energy 2022;47:23731−23750. [CrossRef]

[20] Joshi T, Parkash O, Krishan G. Slurry flow characteristics through a horizontal pipeline at different Prandtl number. Powder Technol 2023;413:118008. [CrossRef]

[21] Joshi T, Parkash O, Krishan G. Numerical investigation of slurry pressure drop at different pipe roughness in a straight pipe using CFD. Arab J Sci Engineer 2022;47:15391−15414. [CrossRef]

[22] Joshi T, Parkash O, Murthy AA, Krishan G. Numerical investigation of Bi-model slurry transportation in a straight pipe. Results Engineer 2023;17:100858. [CrossRef]

[23] Parkash O, Kumar A, Sikarwar B. CFD modeling of slurry pipeline at different Prandtl numbers. J Therm Engineer 2021;7:951−969. [CrossRef]

[24] Seddeek MA, Odda SN, Akl MY, Abdelmeguid MS. Analytical solution for the effect of radiation on flow of a magneto-micropolar fluid past a continuously moving plate with suction and blowing. Comput Mater Sci 2009;45:423−428. [CrossRef]

[25] Akinbo BJ, Olajuwon BI. Effects of heat generation/absorption on magnetohydrodynamics flow over a vertical plate with convective boundary condition. Eur J Comput Mech 2021;4-6:431−452. [CrossRef]

[26] Hayat T, Asad S, Mustafa M, Hamed HA. Heat transfer analysis in the flow of Walters' B fluid with a convective boundary condition. Chin Phys B 2014;23:084701−084707. [CrossRef]